

Adsorption of As (III) from Contaminated Water on Activated Carbon-supported Nanoscale zero-valent Iron Particles

Fisseha A. Bezza*, Evans M. Nkhalambayausi Chirwa

Water Utilization and Environmental Engineering Division, Department of Chemical Engineering, University of Pretoria, Pretoria 0002, South Africa
 fissehaandualem@gmail.

Arsenic (As) contamination is a major concern due to its toxicity and tendency to accumulate and bio-magnify within the food chain, causing wider damage to the ecosystem. In the current study, activated carbon-supported nanoscale zerovalent iron (AC-nZVI) particles, were produced using chemical reduction of ferric chloride hexahydrate in the presence of activated carbon as a scaffold to avoid agglomeration and improve their dispersity. Detailed transmission electron microscopy (TEM), and scanning electron microscopy (SEM) characterization of the as-synthesized nanoparticles showed monodispersed nanoparticles of approximate size 45 ± 10 nm. Their potential application for removal of As(III) from contaminated water was investigated in batch adsorption experiments at various adsorbent dosages and pH values. The results of the study demonstrated that AC-nZVI particles exhibited 82.5% removal of As (III) ions (initial concentration 100 mg/L) at an adsorbent dosage of 2 g/L. The adsorption performance increased with increasing adsorbent dosage and removed 99% As(III) at an adsorbent dosage of 5g/L. The Langmuir and Freundlich adsorption models were fitted to the experimental data, and it was found that the Langmuir isotherm fitted the data better than the Freundlich isotherm with a maximum adsorption capacity of 27.83 mg/g of adsorbent. In the current study As(III) exists predominately as uncharged species $H_3AsO_3^0$ under the designed pH range of 4-8, therefore the effects of solution pH on As (III) adsorption were hardly observed. The results of the study demonstrated that activated carbon-supported zerovalent iron particles can have tremendous potential application for the effective removal of As(III) from industrial wastewaters.

1. Introduction

With the rapid development of industries such as metal plating facilities, mining operations, fertilizer industries, tanneries, paper industries, pesticide industries, etc., an increasing amount of heavy metals is directly or indirectly discharged into the environment. Unlike organic contaminants, heavy metals are not biodegradable and tend to accumulate in living organisms and many of the heavy metal ions are known to be toxic or carcinogenic. Toxic heavy metals of particular concern in industrial wastewaters include zinc, copper, nickel, mercury, arsenic, cadmium, lead, and chromium (Fu *et al.*, 2011). Out of these heavy metals, arsenic is found to pose maximum adverse effects on human health via arsenic-contaminated drinking water. Arsenic is one of the most widespread and significant water contaminants originating from the earth's crust. Because of its ubiquitous nature and high natural abundance, a large portion of the human population drinking arsenic-contaminated water is at risk, especially in developing countries that have limited water treatment facilities. Arsenic is introduced into the environment through natural processes (weathering reactions, volcanic emissions) as well as anthropogenic activities (Smedley *et al.*, 2001).

The natural occurrence of As in groundwater is of great concern due to the potential detrimental effects to human health, especially through chronic exposure over an extended period. Contamination of groundwater, either from anthropogenic or natural sources with several health impacts, has become a major environmental concern in different parts of the world. Millions of people in several countries are exposed to high levels of As via intake of As-rich groundwater (Shankar and Shanker, 2014). On a worldwide scale, it has been estimated that over 137 million people in more than 70 countries are affected by arsenic poisoning of drinking water

(Ramos *et al.*, 2009). Arsenic is linked to the development of various forms of cancer such as skin, bladder, liver, and lung cancer (Chen *et al.*, 1992). Aside from being carcinogenic, arsenic has also been linked to non-cancerous multi-systemic health issues such as dermal diseases, cardiovascular disease, hypertension, and diabetes mellitus (Cantu *et al.*, 2016). Considering its toxicity, the World Health Organization (WHO) has set a maximum guideline concentration of 0.01 mg/L for As in drinking water (Yamamura *et al.*, 2003). Arsenic exists in groundwater predominantly as inorganic arsenite, As(III) (H_3AsO_3 , $\text{H}_2\text{AsO}_3^{1-}$, HAsO_3^{2-}), and arsenate, As(V) (H_3AsO_4 , $\text{H}_2\text{AsO}_4^{1-}$, HAsO_4^{2-}) (Manning *et al.*, 2002). Greater attention is required for the removal of As(III) from groundwater due to its higher toxicity and mobility, which mainly arises from its neutral state (HAsO_3^0) in groundwater as compared to the charged As(V) species (H_2AsO_4^- , HAsO_4^{2-}), which predominate near pH 6-9 (Kanel *et al.*, 2005). Because of the high affinity of arsenic for protein, both trivalent and pentavalent forms of arsenic readily accumulate in living tissues. In its lower oxidation state, Arsenic As(III) is more toxic and mobile than arsenic in the higher oxidation state As(V).

Several remediation methods such as coagulation and flocculation, adsorption, biosorption, ion exchange, and membrane filtration have been employed to mitigate arsenic and other heavy metal contamination in groundwater (Babaee *et al.*, 2018). Although these methods are effective for remediation of arsenic they have significant disadvantages, including high energy requirements, inefficient metallic ion removal, generation of toxic sludge, and cost of equipment (Babaee *et al.*, 2018). However, adsorption evolved as the most promising method among the available methods as this method does not add undesirable by-products and the used adsorbents can be regenerated for reuse up to a reasonably good number of cycles (Cheng *et al.*, 2021). Adsorbents like activated alumina (AA), activated carbon (AC), copper-zinc granules, and granular ferric hydroxide have been used to remove arsenic from contaminated water (Ramos *et al.*, 2009).

Recently, nanoscale zero-valent iron (nZVI) has gained an increasing familiarity owing to its environmental benignity, cost-effectiveness, large specific surface area, and high reduction capacity toward a broad range of organic and inorganic contaminants in aqueous solutions (Vilardi *et al.*, 2017; Zhang *et al.*, 2019; Cheng *et al.*, 2021). The extremely small size of nZVIs, typically in the range 1 to 100 nm, generates a large surface area-to-volume ratio, providing them with an enhanced surface reactivity and more available adsorption sites in comparison with micro-sized materials (Ramos *et al.*, 2009; Babaee *et al.*, 2018). However, nZVI particles have a strong tendency to aggregate to form larger clusters or chains in the micrometer scale, which subsequently leads to a significant and rapid loss in reactivity and decreases its mobility. In order to be effective, nZVI particles thus need to be in the form of stable dispersion in water so that they can be delivered to the water-saturated porous material in the contaminated areas (Hotze *et al.*, 2010). Several studies have reported surface modification of nZVI by polymers and surfactants, clay, and activated carbon which provides steric and electrostatic stabilization against the particle-particle attractive forces and significantly improves its transport in porous media (Phenrat *et al.*, 2008). Activated carbon, zeolite, montmorillonite, bentonite, kaolin, and reduced graphene oxide (rGO) have been reported to support nZVI dispersed growth and avoid agglomeration (Cheng *et al.*, 2021). Compared to other materials, activated carbon possesses excellent properties such as large specific surface area, small bulk density, high stability, low costs, and strong adsorption capacity (Zhang *et al.*, 2019). Even though activated carbon itself is an efficient adsorbent for arsenic, further modification of the surface by ferrous, ferric iron and zerovalent iron nanoparticles would enhance the adsorption potential of the adsorbent for the removal of arsenic (Zhu *et al.*, 2009). Because of the porous structure and large surface area, activated carbon-supported nZVI particles (AC-nZVI) have higher ability to adsorb arsenic ions and serve longer lifespan than bare nZVI, making them more effective remediation agents for heavy metal-contaminated soil and aqueous media (Liang *et al.*, 2022). In the current study, activated carbon-supported nanoscale zero-valent iron (nZVI) particles were produced using chemical reduction of ferric chloride hexahydrate ($\text{FeCl}_3 \cdot 6\text{H}_2\text{O}$) in the presence of finely ground activated carbon as a support material. The adsorption potential of the activated carbon-supported nZVI (AC-nZVI) for removal of As (III) from contaminated water was investigated.

2 Materials and Methods

2.1 Synthesis of activated carbon-supported nanoscale zero-valent iron (nZVI) particle

Activated carbon-supported nZVI (AC-nZVI) were synthesized using NaBH_4 reduction as previously described by Jin *et al.* (2015). Briefly, 10 g of ferric chloride hexahydrate ($\text{FeCl}_3 \cdot 6\text{H}_2\text{O}$) was dissolved in 50 mL of distilled water and 2 g of finely ground-activated carbon (AC) was added under vigorous stirring in a nitrogen atmosphere at room temperature. The mixture was stirred for 15 min in a nitrogen atmosphere, and then freshly prepared 1.8 M NaBH_4 solution (100 mL) was added drop by drop into the mixture under vigorous and continuous stirring. Vacuum filtration was employed to collect AC-nZVI particles, and these were quickly rinsed three times with absolute ethanol. Then they were dried at 333 K under vacuum and kept in the nitrogen atmosphere prior to

application. The nanoparticles were characterized by transmission electron microscopy (TEM), and scanning electron microscopy (SEM).

2.2 Characterization of activated carbon-supported nanoscale zero-valent iron (nZVI) particles

The prepared AC-nZVI particles were characterized by transmission electron microscopy with energy dispersive X-ray analyser (TEM-EDX), and scanning electron microscope (SEM). The average particle diameter and size distribution were calculated using Java image tool software (ImageJ), based on the data of an average of 80–100 particles. The SEM images of samples were obtained from JEOL Scanning Microscope JSM-6400.

2.3 Batch adsorption studies

Batch experiments were conducted to analyze the effects of the process parameters pH (3–8), and adsorbent dosage (0.25–5 g/L) on As (III) adsorption. The experiments were carried out using 250 mL Erlenmeyer flasks at ambient temperature and pH 7 (unless otherwise indicated). 1000 mg/L of As (III) stock solution was prepared by dissolving an accurately weighed amount of arsenic salt in 1 L of DI water. Solutions of desired concentrations were obtained by successive dilution of the stock solution.

To investigate the effect of adsorbent dosage, an experiment was carried out for 3 h with initial concentrations of 100 mg/L of As (III) and increasing dose of the adsorbent (0.25, 0.5, 1, 2, 4, and 5 g/L). The flasks were shaken with an orbital shaker; operated at 200 rpm for 3 h. Control experiments were conducted in the absence of nanoparticles but under otherwise identical conditions. At predetermined time intervals, suspensions were withdrawn, centrifuged at 5000 rpm for 5 min, and filtered through 0.22 μm syringe filters for analysis.

The adsorption isotherm studies were conducted using an adsorbent dosage of 4g/L with altering As(III) initial concentration (5–100 mg/L) at room temperature and pH 7; time = 3 hours). To study the effect of pH on As(III) removal efficiency, pH of the arsenic solution was adjusted to values in the range of (3–8) by adding 0.1 M NaOH and HCl. At predetermined time intervals, samples were withdrawn and centrifuged for 10 min (12000 rpm) to separate the adsorbent, leaving only dissolved arsenic in the solution. The aliquots were syringe filtered and analyzed for arsenic remaining in the aqueous phase. The residual arsenic was determined using graphite furnace atomic absorption spectrometer (Buck Scientific Model 210 VGP). All experiments were performed in duplicates and the averages were reported. The amount of As (III) adsorbed at equilibrium, q_e (mg/g), was calculated using equation (1) by replacing q_t and C_t by q_e and C_e , respectively.

$$q_t = \frac{(C_0 - C_t)V}{M} \quad (1)$$

Where C_0 = initial concentration of As III (mg/L); C_t = concentration of As III at time t (mg/L); V = volume of the solution (L) and M = mass of dry adsorbent (g) (Nur *et al.*, 2014).

The adsorption data were treated with both Langmuir and Freundlich isotherm models.

The non-linear expression of Langmuir isotherm model can be illustrated as Equation (2) (Nur *et al.*, 2014)

$$q_e = \frac{q_{\max} K_L C_e}{1 + K_L C_e} \quad (2)$$

The non-linear expression of Freundlich isotherm model can be illustrated as Equation (3) (Nur *et al.*, 2014):

Where C_e = equilibrium concentration of As (III) (mg/L), q_e = amount of As (III) adsorbed per unit mass of adsorbent (mg/g), q_{\max} = maximum amount of As (III) adsorbed per unit mass of adsorbent (mg/g); K_L = Langmuir constant related to the energy of adsorption (L/mg)

$$q_e = K_F C_e^{1/n} \quad (3)$$

C_e = equilibrium concentration of As (III) (mg/L), q_e = amount of As (III) adsorbed per unit mass of adsorbent (mg/g), K_F and n = Freundlich constants (mg/g) (K_F is related to the As (III) adsorption capacity of the adsorbent).

3. Results and discussion

3.1 characterizations of the nanoparticles

Figures 1a and b present the transmission electron microscopy (TEM) images of activated carbon-supported nanoscale zero-valent iron particles. The size of activated carbon-supported nanoscale zerovalent iron (nZVI) particles was within the range of 45 ± 10 nm. In contrast, bare nanoparticles synthesized in the absence of the activated carbon displayed larger dendritic floc-like morphology with particle sizes ranging between 500 and 1000 nm. Similarly, the SEM images displayed well dispersed, carbon supported nanoparticles in Figure 2c, while particle agglomeration and increased growth was observed in particles produced in the absence of the activated carbon (Figures 1d), confirming the TEM results. Nanoparticles display their particular properties only

when particles are in dispersed form, thus stable dispersion of the nanoscale zero-valent iron particles in the activated carbon matrix is critical for the efficient sorption of pollutants. Aggregation of nZVI particles (attributable to van der Waals and magnetic forces), decreases nZVI reactivity, mobility, and their adsorption efficiency (Phenrat *et al.*, 2008). In the current study nZVI particle synthesis in the presence of the activated carbon prevented aggregation and assisted in the formation of well-dispersed and size-controlled nZVIs.

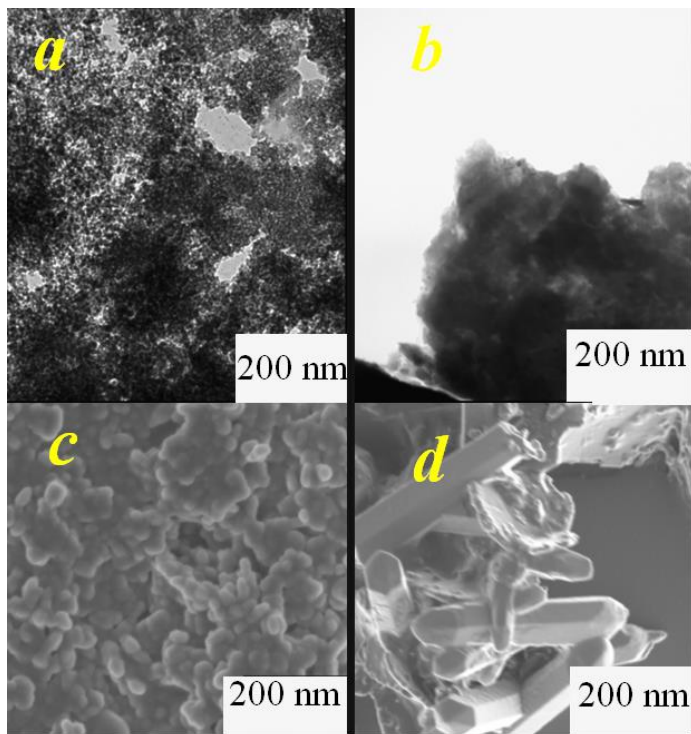


Figure 1: TEM images of: (a) Nanoscale zero-valent iron (nZVI) particles synthesized in the presence of the activated carbon (b) synthesized in the absence of the activated carbon. SEM images of: (c) Nanoscale zerovalent iron (nZVI) particles synthesized in the presence of the activated carbon (d) zero valent Iron particles synthesized in the absence of the activated carbon. The scale bar for the images is 200 nm.

3.2 Effect of adsorbent dose on adsorption of As (III) on zero valent iron nanoparticles

The adsorbent dose is an important parameter in adsorption studies because it gives an idea of the efficiency of adsorbent. Figure 2a presents the adsorption of As (III) at adsorbent dosages of 0.25–5 g/L. It was observed that the percentage of As (III) removal increased with the increase in adsorbent dose. Such a trend is mostly attributed to an increase in the adsorptive surface area and the availability of more active adsorption sites (Uma *et al.*, 2013). Figures 2c and 2d display that both Langmuir and the Freundlich isotherm models fit well with the experimental data. As presented in Table 1, the adsorption data are better fitted by the Langmuir model ($r^2 > 0.989$) compared to the Freundlich model ($r^2 > 0.955$), with a maximum adsorption capacity of 27.83 mg/g. This demonstrates that the adsorption involved the formation of a monolayer on a homogeneous surface. Freundlich isotherm constant can be used to explore the favorability of the adsorption process (Liu and Wang, 2013). When the value of n is within $1 < n < 10$, it is favorable adsorption (Liu and Wang, 2013). As presented in Table 1, the value of n is in the range of 1–10, demonstrating that it is favorable for the adsorption process.

3.3 Effect of pH on adsorption of As (III) on zero valet iron nanoparticles

Solution pH can have a significant influence on the adsorption of heavy metals, due to metal speciation, surface charge, and functional group chemistry of the adsorbent (Kim *et al.*, 2013). As shown in Figure 2b, the adsorption of As (III) at pH 3 was ~ 42% and increased to approximately 97.5% at pH 4, and kept slightly increasing to 99% at pH 8. Varying the initial pH had a small effect on As(III) removal efficiency in the pH range of 4– 8 (Figure 2b); removal ranged from 97.5% when the initial pH was 4 to 99% when it was 8. The pH-dependent behavior can be explained by ionization of both the adsorbate and the adsorbent causing repulsion at the surface and decreasing the net As(III) adsorption. Below pH 9.2, undissociated arsenious acid ($H_3AsO_3^0$) is the predominant species and presumably the major species being adsorbed. When the pH is above 9.2, $H_2AsO_3^-$ is the

predominant As(III) species while the nZVI corrosion product surfaces are also negative (Fe(III)-O-) causing electrostatic repulsion (Kanel *et al.*, 2005). Thus, the adsorption of the neutral H_3AsO_3 , which is the dominant As(III) species at a wide pH range of 2 to 9, would be less strongly influenced by the anion repulsion forces that would likely play an important role in the adsorption of As(V) species at high pH. The lower adsorption at pH 3 may be attributed to the increased solubility of FeOOH at low pH (Zeng, 2004).

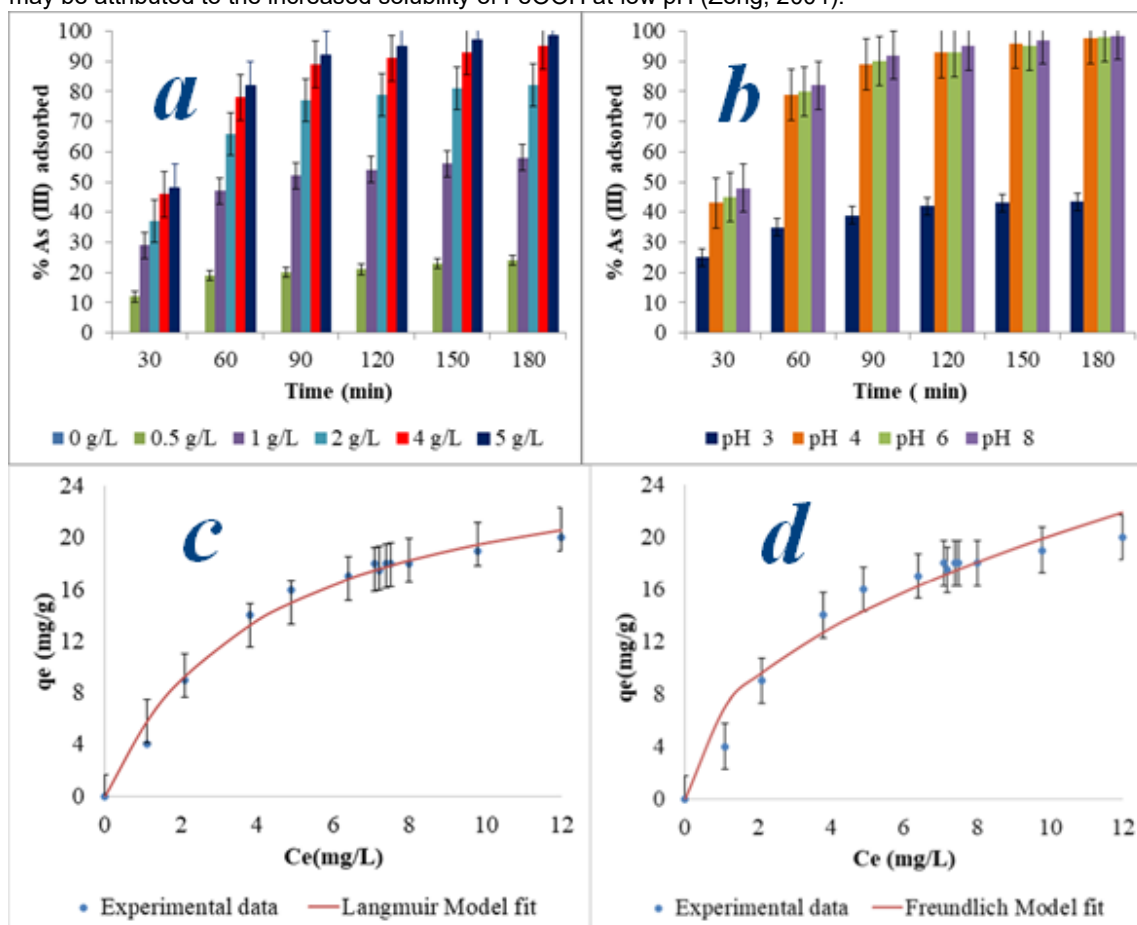


Figure 1: Percentage of As (III) adsorbed at various adsorbent dosages and pH7 (a); at various pH values with 5 g/L adsorbent dosage and an initial As (III) concentration of 100 mg/L (b); Non-linear curve fitting of Langmuir (c) and Freundlich isotherm (d) models at an adsorbent dosage of 4g/L and pH 7.

Table 1: Langmuir and Freundlich isotherm parameters obtained by nonlinear fitting of adsorption data

Model	Parameters	Values \pm SD
Langmuir	q_{max}	27.83 ± 0.90
	K_L	0.239 ± 0.02
	r^2	0.989 ± 0.04
Freundlich	K_F	6.760 ± 0.09
	n	2.110 ± 0.01
	r^2	0.955 ± 0.07

4. Conclusion

In conclusion, a highly reactive activated carbon-supported nanoscale zero-valent iron was synthesized to be used for adsorption of As(III) from contaminated water. The activated carbon-supported nZVIs showed efficient adsorption of As (III) at increasing dosages of the adsorbent within the pH ranges of 4 to 8 while the adsorption

efficiency was adversely affected at pH 3, which may be attributed to the solubility of iron nanoparticles at pHs lower than 3. The study suggests that use of activated carbon as a scaffold is a promising and sustainable option for the synthesis of zerovalent iron nanoparticles loaded on activated carbon with narrow size distribution and high adsorption potential. The synthesis and application of activated carbon-supported zerovalent iron nanoparticles is an attractive and sustainable approach as it is environmentally sound and cost-effective.

References

- Babae Y., Mulligan C.N., Rahaman M.S., 2018, Removal of arsenic (III) and arsenic (V) from aqueous solutions through adsorption by Fe/Cu nanoparticles, *Journal of Chemical Technology & Biotechnology*, 93, 63-71.
- Cantu J., Gonzalez L.E., Goodship J., Contreras M., Joseph M., Garza C., Eubanks T.M., Parsons J.G., 2016. Removal of arsenic from water using synthetic Fe₇S₈ nanoparticles. *Chemical Engineering Journal*, 290, 428-437.
- Chen C.J., Chen C.W., Wu M.M., Kuo T.L., 1992, Cancer potential in liver, lung, bladder and kidney due to ingested inorganic arsenic in drinking water. *British journal of cancer*, 66, 888
- Cheng Y., Dong H., Hao T., 2021, CaCO₃ coated nanoscale zero-valent iron (nZVI) for the removal of chromium (VI) in aqueous solution, *Separation and Purification Technology*, 257, 117967
- Fu F., Wang Q., 2011, Removal of heavy metal ions from wastewaters: a review. *Journal of environmental management*, 92, 407-418
- Halttunen T., 2008, January, Removal of cadmium, lead and arsenic from water by lactic acid bacteria. *Functional Foods Forum*; Department of Biochemistry and Food Chemistry.
- Jin X., Chen Z., Zhou R., Chen Z., 2015, Synthesis of kaolin supported nanoscale zero-valent iron and its degradation mechanism of Direct Fast Black G in aqueous solution, *Materials Research Bulletin*, 61, 433-438.
- Kanel S.R., Manning B., Charlet L., Choi H., 2005, Removal of arsenic (III) from groundwater by nanoscale zero-valent iron. *Environmental science & technology*, 39, 1291-1298.
- Kim S.A., Kamala-Kannan S., Lee K.J., Park Y.J., Shea P.J., Lee W.H., Kim H.M., Oh B.T., 2013, Removal of Pb (II) from aqueous solution by a zeolite–nanoscale zero-valent iron composite, *Chemical Engineering Journal*, 217, 54-60.
- Liang W., Wang G., Peng C., Tan J., Wan J., Sun P., Li Q., Ji X., Zhang Q., Wu Y., Zhang W., 2022, Recent advances of carbon-based nano zero valent iron for heavy metals remediation in soil and water: A critical review. *Journal of Hazardous Materials*, 426, 127993.
- Liu J. and Wang X., 2013, Novel silica-based hybrid adsorbents: lead (II) adsorption isotherms. *The Scientific World Journal*, 2013.
- Manning B. A.; Hunt M.; Amrhein C.; Yarmoff J. A. Arsenic (III) and arsenic(V) reactions with zerovalent iron corrosion products, *Environ. Sci. Technol.* 2002, 36, 5455-5461.
- Nur T., Loganathan P., Nguyen T.C., Vigneswaran S., Singh G. and Kandasamy J., 2014. Batch and column adsorption and desorption of fluoride using hydrous ferric oxide: Solution chemistry and modeling. *Chemical Engineering Journal*, 247, 93-102.
- Phenrat T., Saleh N., Sirk K., Kim H.J., Tilton R.D., Lowry G.V., 2008, Stabilization of aqueous nanoscale zerovalent iron dispersions by anionic polyelectrolytes: adsorbed anionic polyelectrolyte layer properties and their effect on aggregation and sedimentation. *Journal of Nanoparticle Research*, 10, 795-814.
- Ramos M.A., Yan W., Li X.Q., Koel B.E., Zhang, W.X., 2009, Simultaneous oxidation and reduction of arsenic by zero-valent iron nanoparticles: understanding the significance of the core– shell structure. *The Journal of Physical Chemistry C*, 113, 14591-14594.
- Shankar S., Shanker U., 2014, Arsenic contamination of groundwater: a review of sources, prevalence, health risks, and strategies for mitigation, *The scientific world journal*, 2014.
- Uma Y.C. and Sharma U., 2013, Removal of malachite green from aqueous solutions by adsorption on to timber waste. *Int J Environ Eng Mgmt*, 4, 631-638.
- Vilardi G., Stoller M., Verdone N., Di Palma L., 2017, Production of nano Zero Valent Iron particles by means of a spinning disk reactor. *Chemical engineering transactions*, 57, 751-756.
- Yamamura S., Bartram J., Csanady M., Gorchev H.G., Redekopp A., 2003, Drinking water guidelines and standards. Arsenic, water, and health: the state of the art
- Zeng L., 2004, Arsenic adsorption from aqueous solutions on an Fe (III)-Si binary oxide adsorbent. *Water Quality Research Journal*, 39, 267-275.
- Zhang S., Lyu H., Tang J., Song B., Zhen M. and Liu X., 2019, A novel biochar supported CMC stabilized nano zero-valent iron composite for hexavalent chromium removal from water. *Chemosphere*, 217, 686-694
- Zhu H., Jia Y., Wu, X. and Wang, H., 2009. Removal of arsenic from water by supported nano zero-valent iron on activated carbon. *Journal of Hazardous Materials*, 172, 1591-1596